Soil Interaction Model of Hemispherical Sampling Device based on PIV Analysis

Daiki Mori*, Genya Ishigami*

*Department of Mechanical Engineering, Keio University, Japan
e-mail: d.masahi122@z7.keio.jp, ishigami@mech.keio.ac.jp

Abstract

Seeking for microorganisms of extraterrestrial life has been a primary mission on Mars explorations; and there is a possibility of remaining indication of life in Martian subsurface. Therefore, a robotic arm mounted on an exploration robot is required to dig to a certain depth and collect appropriate sample to be analyzed. However, this operation has to be performed with limited power available from solar array panels. In this paper, a hemispherical sampling device is proposed and the soil-device interaction model is formulated applying the Particle-Image-Velocimetry (PIV) analysis and soil mechanics. The interaction model is experimentally validated through sampling tests. The proposed interaction model will be useful for an sampling strategy.

1 introduction

Mars life exploration has been discussed in several space agencies. Trace of life on the Mars is expected to be found deeper than 50 mm subsurface where it is isolated from lethal ultraviolet or it may be behind the rocks, a trace of salt water and place where methane is evaporated. Exploration robots would approach these places of scientific interest and carry out sampling process using its robotic arm. Then the sample would be analyzed with a scientific experiment apparatus mounted on the lander.

Many robotic arms were used for life explorations on the Mars. However, those arms were designed based on its digging ability rather than its energy consumption. The energy used for space robots is mainly supplied from the solar array panel which can only generate up to about six hundred Watt per Martian day. Moreover, the energy generated would dramatically varies along with seasons on the planet. When excavating, the robotic arm has to tolerate relatively large resistance force, resulting in large energy consumption. The Phoenix lander by the NASA reported that it observed 20 N to dig 30 mm below the surface[1].

There are many requirements for robotic arm aimed for space missions. In order to accomplish sampling missions on Mars, there are mainly six types of requirements. Firstly, excavation resistance has to be small enough to reduce energy consumption and to improve the durability of the device. Secondly, less numbers of actuators are better since actuators often malfunction in harsh environment, and therefore, as the third requirements, the mechanical durability is preferred. Fourthly, the device should have an ability to capture dry sand. Chopstick like end-effectors(EE) are, for example, not appropriate for capturing sand. Fifthly, EE has to be capable of digging more than 50 mm subsurface where the microorganism may exist. Finally, the dexterity is required because the sample to be investigated is very small. These are the requirements considered in this paper for developing a sampling tool.

The scope of this work is to establish an energy effi-

Table 1. Requirements and comparisons of possible end-effector design

Requirements	Shovel	Drill	Hand
1. Resistance	△	△	△
2. Number of actuators	○	△	×
3. Durability	○	×	×
4. Scooping ability	○	△	×
5. Digging ability	○	○	×
6. Dexterity	△	△	○

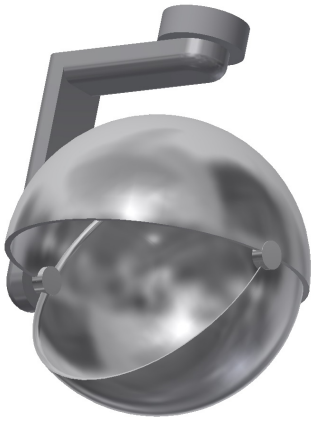

Figure 1. Concept sampling tool

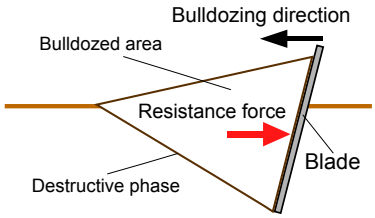

Figure 2. Model of bulldozing resistance

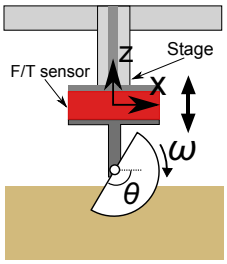

Figure 3. Coordinate

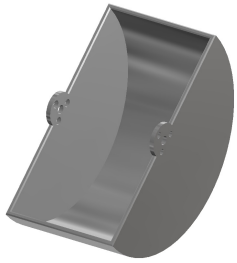

Figure 4. Model type device

cient strategy for soil sampling task with the robotic arm. In this paper, the shape of end-effector is reviewed, then an excavation model is proposed considering the interaction of soil and the tool. The modeling procedure is as follows: first, an energy-efficient EE shape is examined (Section 2), and then, the Particle Image Velocimetry (PIV) is employed to observe the soil deformation profile (Section 3). The soil-tool interaction model is formulated based on the PIV analysis (Section 4), and the model is validated through a sampling tool test bed (Section 5).

2 EE shape review

The robotic arms are expected to dig and carry soil to onboard scientific instrument mounted on the rover or lander. The requirements previously mentioned are listed in Table 1. Here are three possible types of EE are considered: 1. Shovel type 2. Drill type 3. Hand type.

In Tab. 1, the circle represent that the type adequately fulfills the requirement; the triangle represents that the type may manage the requirement with improvement; and the cross represent that it is unable to achieve the requirement. Shovel type can operate with few actuators and its shape is integrated. Also, it can adapt to variety of samples. As for drill types, they are good at digging deep into the soil but its mechanism are more complicated compared to other types, which reduces durability. For hand types, too many actuators are used. Many actuators mean much energy consumption. Therefore, shovel type is the most appropriate shape for sampling on Mars.

Next, resistance reduction and pinpoint sampling is

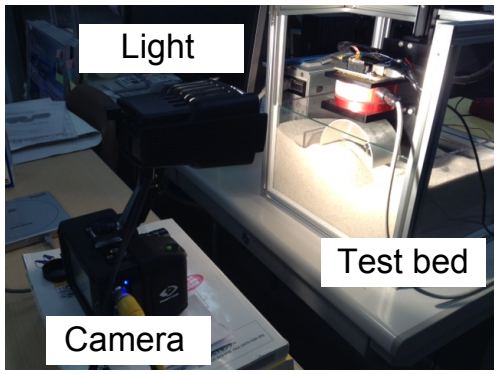

Figure 5. Experiment layout

considered to shape the tool. Major force when excavating is the bulldozing force Fig. 2. Bulldozing resistance occurs when the blade is pushed through the soil. In order to reduce the bulldozing force, circular side cross section is adopted and the rotary shaft is placed in the center of the circle. Furthermore, circular front cross section is applied for pinpoint sampling. With circular front cross section, small amount of sample will be collected when the rotary shaft is lifted from the surface of soil. Combining these two shapes, the hemispherical sampling device was formed (Fig. 1).

The cylindrical sampling device Fig. 4 is used for formulating excavation model in this paper. By layering the cylindrical sampling device with different radius, the model can be applied to hemispherical sampling device. Excavation model for cylindrical sampling device is mainly discussed in this paper.

3 PIV analysis of soil deformation

In the field of soil mechanics, observation was a common attempt to understand the behavior of soil. Observation is also used in this paper to reveal the interaction between soil and the tool using PIV analysis. By applying PIV analysis, soil particle in each frame is followed in order to calculate the velocity of the particle. PIV analysis enables to discuss the deformation in a quantitative way.

3.1 PIV analysis test bed

Test bed is designed to rotate the tool in constant speed and is capable of changing the height of the tool. Fig. 5 shows the layout of the test bed. Sampling tool with one side of the wall taken off is pressed against the glass of the test bed. Using the camera, soil deformation is filmed throughout the excavation sequence. Then, the movie is analyzed by PIVlab [2] (toolbox of MATLAB).

Radius of the tool was set to 50 mm and the height of the rotary shaft was fixed to 20 mm. Dry ”Keisa 5” was

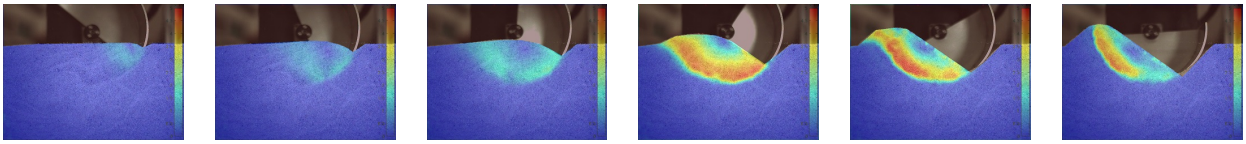

(a)Frame 1 (b)Flame 2 (c)Flame 3 (d)Frame 4 (e)Flame 5 (f)Flame 6

Figure 6. PIV with absolute scale

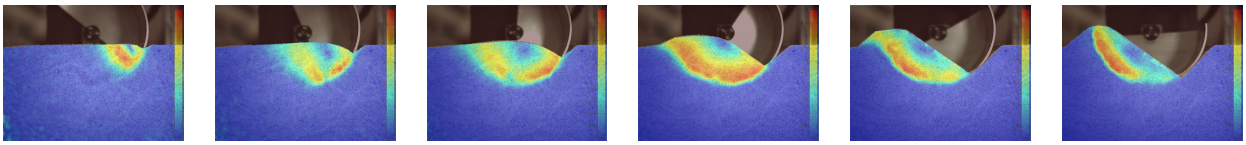

(a)Frame 1 (b)Flame 2 (c)Flame 3 (d)Frame 4 (e)Flame 5 (f)Flame 6

Figure 7. PIV with frame-relative scale

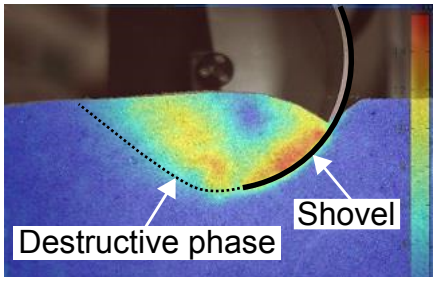

Figure 8. Destructive surface of soil

used to represent sample and the frame rate was set to 5 fps. Fig. 3 shows the coordinate system.

3.2 PIV Experiment result

Fig. 6 shows the result of PIV analysis with color scale fixed throughout the process. On the other hand, Fig. 7 shows the result with color scale distributed within each frame. Red part represent the fastest particle and blue represent static particle.

Fig. 6 indicates that small soil deformation occurs in the first half of excavation, and large deformation in the last half. From Fig. 7, the border of static soil and deforming soil can be seen throughout the process. This is called destructive phase and Fig. 8 shows it with label. Destructive phase is discussed in the theory of passive earth pressure in the field of soil mechanics. Therefore, the theory of passive earth pressure can be applied to the excavation model.

3.3 Soil deformation

Soil deformation process was determined geometrically based on PIV analysis. This is used for passive earth pressure discussed later in excavation model.

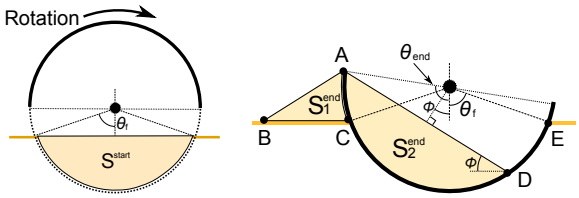

(a) Start (b) End

Figure 9. Soil form change

Fig. 9 shows the deformation of soil at start and at end. θ_{end} can be derived from the equation below.

$$S^{start} = S_1^{end} + S_2^{end} \quad (1)$$

Each area can be calculated using the angle shown in Fig. 9. Soil formation is defined using the final configuration.

4 Excavation model

In order to formulate the excavation model, soil mechanics and terramechanics were adopted. Soil mechanics are applied to static issues and terramechanics are applied to moving soils. There are studies about wheel loader, and the scooping model has been proposed in [8][9]. However, those studies are mostly about rock piles which behaves very differently compared to Martian soil. Martian soil consist of smaller particles and are dry. Discrete-Element-Method(DEM) maybe another solution to calculate the resistance [10], but defying enormous amount of particles for DEM calculation would not be a suitable method for Martian soil. Therefore, excavation model is established with the theory as previously explained.

First, forces acting on the tool were categorized as shown in Fig. 10. F_1 is force acting on bottom upper

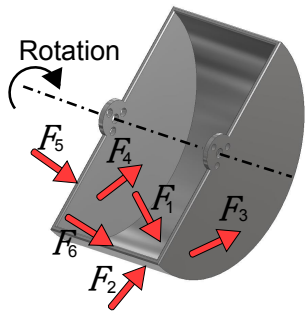

Figure 10. Force model

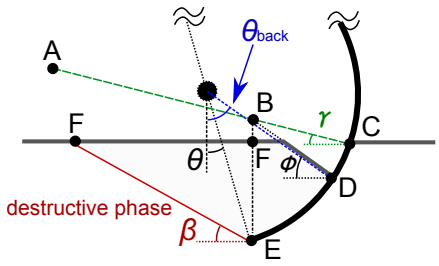

(a) Angle definition

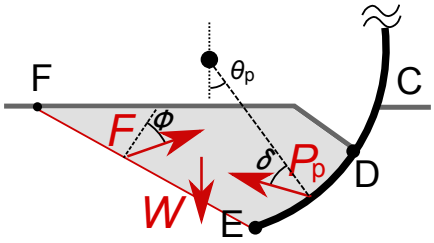

(b) Force direction

Figure 11. F_1 Rotation first half

surface, F_2 is force acting on bottom lower surface, F_3 is force acting on side outer surface, F_4 is force acting on side inner surface, F_5 is force acting on side edge andF_6 is force acting on bottom edge. Model for each force is formulated in the following sections.

4.1 F_1: Bottom upper surface

F_1 is the most dominant force among the forces. This force derive from the resistance when the blade is pushed through the soil. This is called bulldozing force and is formulated by Bekker and Hegedus[5]. However, this model is only capable of calculating the resistance when the soil is in static condition. Thus, bulldozing resistance in unstatic state is proposed.

The model in the first half of excavation is formulated. Angles are defined as shown in Fig. 11(a). ϕ is internal friction angle of sample, β is destructive phase angle, θ_{back} is the rearmost soil contact angle. g is gravitational acceleration, ρ is density of soil and w is tool width. S_{sand} is the area of soil from side cross section. The weight W is calculated by $W = S_{sand} \cdot \rho g$.

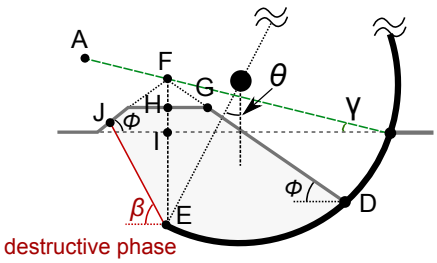

(a) Angle definition

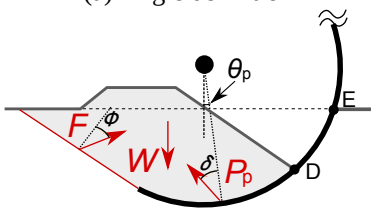

(b) Force direction

Figure 12. F_1 Rotation last half

Next, equilibrium of three forces, weight, passive earth pressure and resistance at destructive phase was considered. Direction of each force is as shown in Fig. 11(b). θ_p is defined as follows.

$$\theta_p = \frac{\theta + \theta_{back}}{2} \tag{2}$$

By applying sine theorem, P_p is calculated by the equation bellow.

$$P_p = \frac{\sin(\phi + \beta)}{\sin(\pi - \theta_p - \delta - \phi - \beta)} \cdot W \tag{3}$$

P_p is dependent on variable β. In Coulomb's passive earth theory, β with smallest P_p is adopted[3]. This is because destructive phase with less energy appears first within the soil.

Next, model in the last half of excavation is formulated. Angles are defined as shown in Fig. 12(a) and the weight of soil is calculated. Then this weight is applied to equation (3). However, θ_{end} is calculated differently.

$$\theta_p = \theta_p(\pi/2) + (\pi/2 + \phi - \theta_p(\pi/2)) \cdot \frac{\theta}{\phi} \tag{4}$$

P_p is formulated by dividing the excavation process into two parts. Important point is that P_p is the total force acting on the soil which derives from the tool. Thus it is possible to include F_4 in P_p.

4.2 F_2: Bottom lower surface

According to Fig. 13(a), no movement can be identified under the bottom blade of the tool. Supposing that

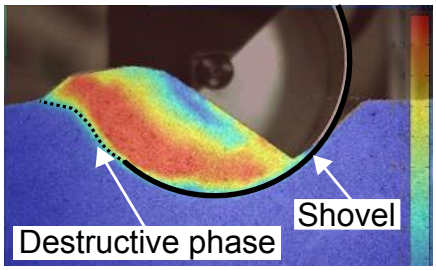

(a)Soil Movement

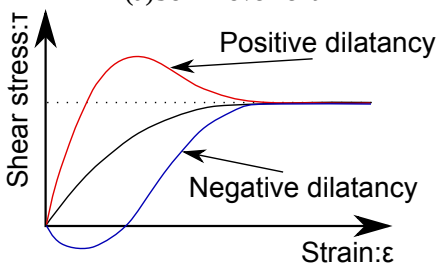

(b)Soil dilatancy

Figure 13. Phenomina under the tool

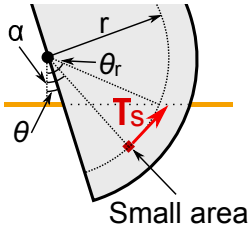

Figure 14. Side surface

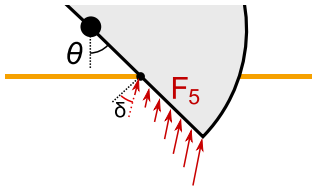

Figure 15. sideedge

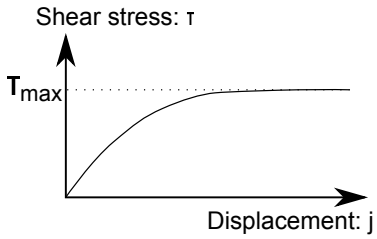

Figure 16. Shear stress curve

some kind of force is acting against the tool, at least a small velocity field must occur. Therefore, dilatancy effect is considered. Dilatancy is a phenomena shown in Fig. 13. Very small force would occur so F_2 does not require formulation.

4.3 F_3: Side outer surface

Shear stress is acting as resistance on the side outer surface of the tool. In order to calculate total shear stress, first, force acting on small area is formulated(Fig. 14).

$$\sigma = (r\cos\alpha - h_0)\rho g \tag{5}$$

The static earth pressure is calculated as shown above. Then this pressure is applied to stress-displacement curve by Janosi,Hanamoto(Fig. 16). τ_{max} is the maximum shear stress, j is soil displacement, k is deformation parameter, c is soil adhesion, σ is vertical pressure and the equilibrium is as shown below.

$$\tau_s(r,\alpha) = \tau_{max}(1 - e^{-j/k}) \tag{6}$$

$$\tau_{max} = c + \sigma\tan\phi \tag{7}$$

$$j = R(\alpha - \theta) \tag{8}$$

By integrating the force, total force is calculated.

$$\mathbf{F_3} = \int_{h_0}^{R}\int_{\theta_r}^{\theta}\tau(r,\alpha)d\alpha\cdot dr \tag{9}$$

4.4 F_5: Side edge

Plate sinkage pressure equation formulated by Bekker is applied as a side edge resistance. The equation is as follows:

$$p(h) = \left(\frac{k_c}{b} + k_\phi\right)h^n \tag{10}$$

k_c and k_ϕ are cohesive and friction moduli of deformation. Direction of this sinkage pressure is angled as shown in Fig. 15. With w(edge thickness) and q (pressured rate of edge), F_5 is formulated as follows.

$$F_5 = \int_{h_0}^{R\cos\theta}\left(\frac{k_c}{b} + k_\phi qw\right)\frac{h^n}{\cos\theta}dh \tag{11}$$

4.5 F_6: Bottom edge

In Fig. 8, soil around the tip of the tool is not effected. If there is any kind of affection by the tool, there must be a velocity field in a radial fashion. However, this cannot be identified so F_6 can be included in P_p.

4.6 Total force

Each force was formulated as previously stated. To calculate the total force, first, final deformation shape was determined. Then, P_p, F_3 and F_5 were calculated and were added together. As for the characteristics of the calculated force, F_5 was the dominant in the first half of excavation and P_p became dominant in the last half.

5 Model validation experiment

In order to validate the excavation model, experiment was performed. Resistance was determined using force sensor attached to the tool. Also rotation speed was stabilized using PID control. First, speed dependency of the tool was examined and then experiment results and model calculation results were compared.

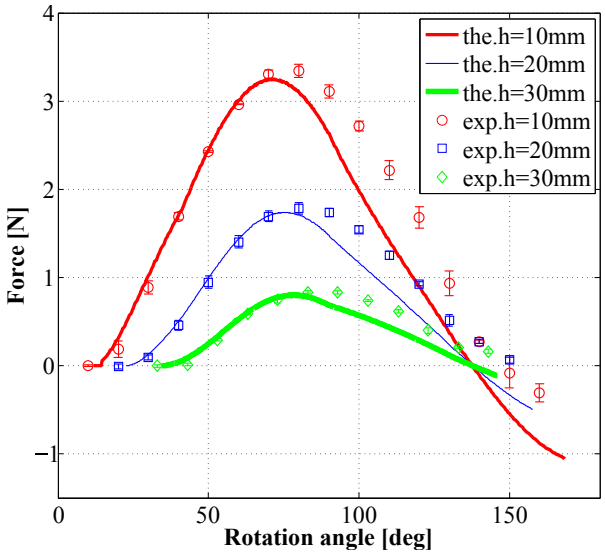

(a) Force (X axis direction)

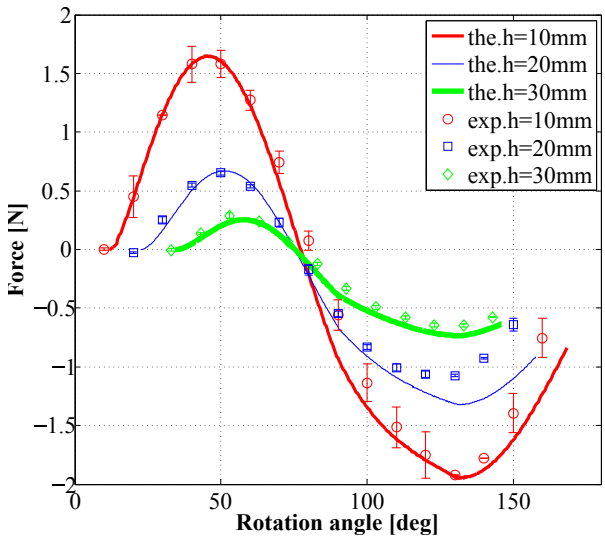

(b) Force (Z axis direction)

Figure 17. Force with differernt tool height

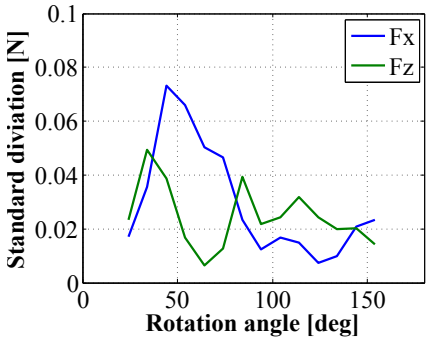

Figure 18. Results from three different speed

5.1 Velocity dependency

Rotation speed of the tool is not considered in the model proposed in this paper but actuator speed has a big influence on energy consumption so it requires research. Excavation experiment was conducted in three different rotation speed: 3 deg/s, 5 deg/s and 7 deg/s. Standard deviation was calculated and the maximum was 0.07 N. This is about 3 % of peak resistance so it can be concluded that the model does not require consideration of rotation speed.

5.2 Model validation

Fig. 17 is the comparison of model calculation and experiment results. X axis force increase in the first half of excavation and decreases in the last half. This drives from the increasing passive earth pressure during the first half when the tip of the tool is going into the soil, and reducing bulldozing force while the tip is moving towards the surface. On the other hand, Z axis force has a upward resistance in the first half and downwards resistance in the last half.

Table 2. RMS errors between the measured and estimated forces

Height(mm)	10	20	30
F_x (N)	0.2492	0.4477	0.1110
F_z (N)	0.1802	0.1626	0.029

According to Fig. 17, model calculation qualitatively has the same characteristics as the experiment results. Tab. 5.1 shows the RMS values of each height against model calculations.This table indicated that the excavation model agrees well with experiment results. On the other hand, error gradually increases in the last half. This is because soil mechanics theory applied to the model is for static soil and not for deforming soil. However, excavation model is adequately showing the same tendency to experiment result in order to consider manipulation strategy.

5.3 Force curve and efficiency curve

Fig. 19 is the force direction curve representing the direction of the force acting on the tool through the excavation process. This diagram indicates the force vector acting on the sampling device. The force couple of F_x and F_z shows the magnitude of the resistance force and

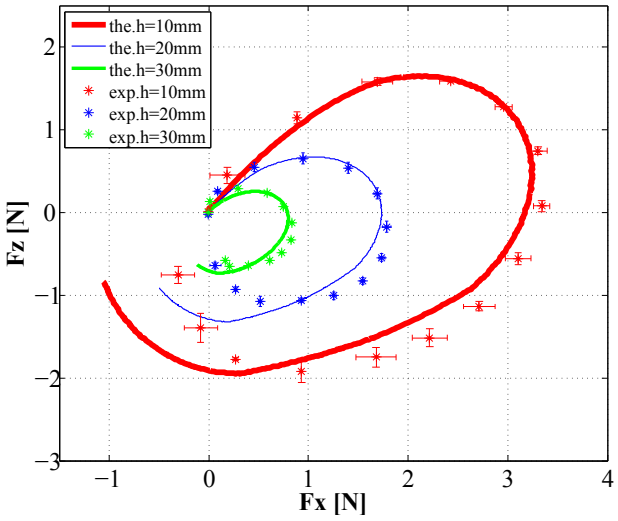

Figure 19. Force direction curve

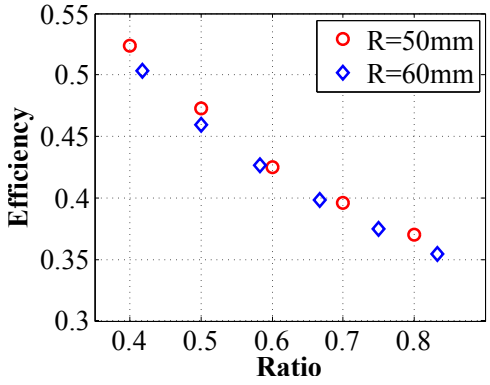

Figure 20. Efficiency with different tools

the angle relative to the horizontal (= $\tan^{-1}(F_z/F_x)$) gives the direction of the resistance force. Therefore, based on the values of the vector, an energy-efficient sampling approach will be elaborated.

Smapling tool efficiency can be defined with mass of sample as shown in Fig. 20. X axis represent ratio between excavation and tool radius. Efficiency is calculated by (Soil weight)/(Total resistance). This graph indicates that excavating shallow soil with tool of large radius has better efficiency. This is one of the way to calculate the efficiency of the sampling device.

6 Conclusion

In this paper, the energy efficient sampling tool has been proposed and the soil-tool interaction model has been formulated based on the PIV analysis. Furthermore, in the experiment, the model well agrees with the experimental results. Also, the force direction curve has been shortly proposed.

The excavation model will be useful for the design of the most energy-efficient size of the tool once a target depth of soil sampling is determined. Also, the EE resistance vector can be exploited for a control of robotic arm, taking into account the manipulability with regard to the force vector.

References

[1] R. E. Arvidson, et al.; “Results from the Mars Phoenix Lander Robotic Arm experiment,” *Jounal of Geophysical research, vol. 114, E00E02,* 2009.

[2] http://pivlab.blogspot.jp (as of December 2013)

[3] F. Oka, “Soil mechanics” Asakura Syoten, 2003.

[4] Z. Janosi and B. Hanamoto,; “The analytical determination of drawbar pull as function of slip for tracked vehicle,” *Proc. of the 1st Int. Conf. on Terrain-Vehicle Systems,* Torio, 1961.

[5] Bekker, M. G. : “Introduction to Terrain-Vehicle Systems”, The University of Michigan Press, 1969

[6] A.R.Reece,; “Principles of Soil-Vehicle Mechanics,” Proceedings of the Institution of Mechanical Engineers, vol.180, part 2A, 1965-1966.

[7] E. Hegedus:“A Simplified Method For the Determination of Bulldozing Resistance”,Department of the army ordnance tank-automotive command research division land locomotion laboratory, report No.61, 1960

[8] H. Takahasi, and Y. Saito, “Analysis on the Resistive Force acting on the Bucket of Power Shovel in the Excavating Task of Piled Fragment Rocks”, Applied Mechanics Proceedings, Vol.7, pp.787-796, 2004

[9] T. Fujiwara, N. Okada, H.Osumi, and S.Sarata,“Estimation of Reaction fro Rock Piles Applying to Wheel Loader”, Proceedings of the 2011 JSME Conference on Robotics and Mechanics, Japan,2011

[10] T.Yoshida, T. Koizumi, N. Tsujiuchi, K. Chen, and N. Nakamoto,“Examination of Effective Improvement in Digging Operation for Hydraulic Excavators”, Proceedings of Japan Mechanical Engineering, Vol.78, Japan, 2012